SEMARAK ILMU PUBLISHING

CFD Letters

Journal homepage:
https://semarakilmu.com.my/journals/index.php/CFD_Letters/index
ISSN: 2180-1363

Improvement of Plate-Fin Heat Exchanger Performance with Assistance of Various Types of Vortex Generator

Ali Sabri Abbas[1], Ayad Ali Mohammed[2,*]

[1] Department of Mechanical engineering, Engineering College, Al Nahrain University, Baghdad, Iraq
[2] Al-Furat Al-Awsat Technical University, Al-Mussaib Technical College, Babylon, Iraq

ARTICLE INFO

Article history:
Received 15 December 2022
Received in revised form 15 January 2023
Accepted 13 February 2023
Available online 1 July 2023

Keywords:
plate fin-heat exchangers; ORT fin; vortex generator; rectangular winglet pair; delta winglet pair; trapezoidal winglet pair; CFD

ABSTRACT

A 3-dimensional incompressible laminar flow and heat-transfer in a plate-fin heat exchanger (PFHE) where investigated numerically in this article. The influence of mounting a longitudinal vortex generator (LVG) on the offset rectangular-triangular fin (ORT) in the PFHE, on thermal and hydro-dynamic fields are presented. The novelty of this study is by attaching a LVG to an offset strip fin (OSF) surface. The cases of study for the PFHE are established, by using a built-in rectangular winglet pair type RWP longitudinal vortex generator carried out and fitted on this fin to improve the convective heat transfer of the (ORT) fin while minimizing pressure loss. The upper and lower plates are exposed to constant heat flux and the working fluid is air where chosen under a laminar range of RE (600 to 1400). The laminar flow and heat-transfer are governed by continuity, momentum and energy equations. ANSYS FLUENT (2021 R1) is used to get the numerical results, based on the finite volume method. The performance of the VG is assessed for an optimum winglet attack angle (45°), as well as by modifying the geometrical size parameters, namely the height and placement (L) of the RWP LVG. The result shows that the Nusselt number reaches its optimum enhancement values by using a common flow up CFU built-in rectangular winglet pair type RWP VG with a height and entrance length of (h=1.25mm, L=0.5mm), by 22.23% as compared with base case configuration (ORT). Finally, a two more LVG are tested with the optimum conditions of the RWP, which they are a delta winglet pair (DWP) and trapezoidal winglet pair (TWP). In addition, the temperature fields for the primary and secondary flows were shown in contour and streamline diagrams.

1. Introduction

The vortex generator surface depends on generating longitudinal vortices that enhance thermal mixing and increase the coefficient of heat-transfer [1]. The gas side coefficient of heat-transfer can be enhanced by interrupting thermal boundary layer growth while simultaneously destabilizing the hydro-dynamic boundary layer using vortex generators. The performance of VGs might be influenced by a variety of factors such as its shape, location, geometry, and attack angle [2].

* *Corresponding author.*
E-mail address: ayadia1@atu.edu.iq (Ayad Ali Mohammed)

https://doi.org/10.37934/cfdl.15.7.131147

The potential of a WPVG for the heat-transfer augmentation in a PFHE, with triangular fins as inserts, was numerically estimated by Gupta *et al*., [3]. The calculations were performed by utilizing the modified MAC approach to solve an unstable, 3-dimensional Navier-Stokes equation and an energy equation. The study demonstrated the flow structure and WPVG efficacy in enhancing heat-transfer. The calculations are performed with REs of 200 and the winglet at an attack angle of 20^{o}. The results showed that the WPVG increases heat transmission by 13 percent. Heat-transfer augmentation with a WPVG is expected for Pr = 0.71, Re = 200-500, and varied heights of the WPVG.

Ganesh *et al*., [4] explored PFHE enhancement of heat-transfer using Modified Fin Surfaces numerically. A steady of an energy equation and a 3-dimensional Navier–Stokes equation were resolved by using the Fluent ANSYS program. The obtained geometry was a PR with built-in DWP VG. For CFD setup, four distinct attack angles (15°, 25°, 35°, and 45°) and different Re-numbers (1000 to 4000) are investigated. According to the findings of the various (β) of the VGs, the performance of the DWP VG at 25° is the best in terms of heat transmission at all Re-number levels.

The performance parameters were estimated in the laminar flow regime concerning the augmentation of heat-transfer by using WVGs in the study of Ebrahimi and Saeid [5]. The numerical computations are performed by solving a steady, 3-dimensional Navier–Stokes equation and an energy equation by using Fluent software program. They studied a pair of delta winglets (DWP) and a pair of rectangular winglets (RWP). The results display that use of LVGs could effectively augment the heat-transfer of the HE. According to the non-dimensional defined parameter for estimation of performance ($Nu_m/Nu_{m,0}$)/(f/f_0), the channel with DWP shows superior overall performance than RWP. The CFD configuration of DWP displays a better overall performance at Re-numbers lower than 720 and the CFU configuration of DWP shows a better overall performance at Re-numbers more than 720. Likewise, the CFD setup outperforms the CFU configuration in terms of overall performance for RWP.

Gupta *et al*., [6] Studied numerically a laminar convection heat-transfer in a PFHE, with triangular fins and VG. The complete energy equation and Navier–Stokes equation are solved by the "Marker and Cell" algorithm using the staggered grid procedure. An RWVG is mounted on the triangular fins. The results displayed that the average Nu increases with an rise in the attack angle and Re. For the same area of the VG, the rise in length of the VG shows more heat-transfer augmentation than increasing the height. A moderate pressure drop comes with an increase in heat transfer.

Khoshvaght-Aliabadi [7] experimentally looked into the impact of vortex-generator (VG) and Cu/water Nanofluid flow on the performance of plate-fin heat exchangers. Based on the testing results, using the VG channel rather than the plain channel increases the heat-transfer rate. Furthermore, the results showed that the VG channel outperformed the Nanofluid in terms of PFHE performance. It is detected that the combination of the two heat-transfer augmentation techniques has a noticeably high thermal-hydraulic performance. Lastly, correlations are established to predict the Nu-number and f-factor of Nanofluids flow inside the VG channel.

Vasudevan *et al*., [8] The research has been done numerically by the "Marker and Cell" method utilizing the staggered grid approach to discuss the enhancement potential of triangular fins with DWP attached on their incline surfaces. It can be shown that a 20-25% increase in heat transmission may be achieved at the price of a minor pressure loss. The amplification of heat transmission is also affected by the DWVG's attack angle. They discovered that triangular fins with attached DWVG (secondary fins) have a lot of potential as inserts (protrusions) within the flow passageways generated by the two adjacent plates in a PFHE. The DWVG might potentially be punched out to make the manufacturing process easier. Stampings are developed on the duct wall in this stage. The flow structure becomes more convoluted, yet heat transmission is much improved.

Sachdeva *et al*., [9] analyzed experimentally the heat-transfer augmentation in a PFHE with triangular fins and a RWVG on its incline surface, using the "Marker and Cell" method to solve the Navier-Stokes and continuity equations. According to the investigation, using a RWVG at a 26° angle of attack leads in a 35% increase in the combined spanwise average Nu-number when compared to the PFHE without any VGs.

Sachdeva *et al*., [10] investigated the performance of the integration of triangular secondary fins and DWVG with stamping on incline surfaces using secondary flow analysis in plate-fin triangular ducts with delta wing vortex generators. The "staggered grid" approach was used to solve the whole Navier-Stokes equation and the energy equation. The findings showed that increasing the DWVG improves the heat-transfer capability of the HE. Heat-transfer rises as Re-number and attack angle increase. There is a parallel rise in the needed pumping power, which increases with greater (β) but reduces with higher Re-number. Stamped DWVG is somewhat less effective than the connected one, but it has the benefit of being easier to manufacture.

Gupta and Kasana [11] examined numerically 3-dimensional simulations on a PFHE (with triangular fins) to estimate the laminar heat-transfer and fluid flow characteristics with LVGs. The results showed that the heat-transfer of the channel was effectively augmented by the application of inline LVGs. Heat-transfer rises even more as the Re number rises from 200 to 500 and the attack angle rises from β = 15° to 22.5°. The calculations are also carried out to determine the ideal site for the second RWP.

The goals of this study can be summarized as investigating how the vortex generators on the ORT fin configuration affect heat transfer to a single-phase fluid in PFHE, and gaining a better and more quantitative understanding of the heat transfer process that takes place when a fluid passes through the ORT fin with aid of vortex generators configuration as follows:

i) To determine the increase in heat transfer on the ORT fins of a plate-fin heat exchanger using a various types winglet pair vortex generator integrated into the fin surfaces.
ii) To investigate the performance of the HE at various geometrical size (height) and position of the RWP at various Re-numbers.
iii) To quantify the optimized geometry of the RWP vortex generator, and the most best winglet pair vortex generator type could be used in the ORT fin geometry.

2. Model Description

A rectangular winglet pair (RWP) on a common flow down (CFD) shape mounted on the surface of a new proposal (ORT) fin from Ref. [12] were studied, as shown briefly in Figure 1. The novelty of this study is presented by attaching a LVG to an offset strip fin (OSF) surface. The plane of the RWP makes with an optimum attack angle (β) with the direction of flow by (45^o) approved by a study [13]. The three leading edges of the RWP are considered at (L = 0.5, 3 and 5mm). Three different heights of the LVG were taken which are (h= 0.75,1 and 1.25mm) by investigating their thermal hydraulic features by exploring its Nussult number (Nu), pressure drop (Δp) and the performance evaluation criterion (PEC). Finally, a two more LVG are tested with the optimum conditions of the rectangular winglet pair (RWP), which they are a delta winglet pair (DWP) and trapezoidal winglet pair (TWP).

For the present study, the three cases of plate-fin heat exchanger fin geometers with the built-in LVG were created on Workbench 2021, the front view of the computational domain for each case is illustrated in Figure 1, Figure 2, And Figure 3. The detailed description for ORT fin geometry proposed by previous study [1] listed in Table 1.

Air enters the PFHE at various laminar Re numbers (velocities), and the exit is through an outflow boundary. A laminar, isothermal, and steady-state condition will be taken into consideration to solve the flow field. Laminar regime was proposed by the previous mentioned studies [5 - 13]. Five Re values, ranging from 600 to 1400, and a fixed Pr number have been covered in the study. Knowing the local heat flux which is 3000 w/m^2 for the upper and lower plates, values of local heat-transfer coefficients along the upper and lower plates allowed for the calculation.

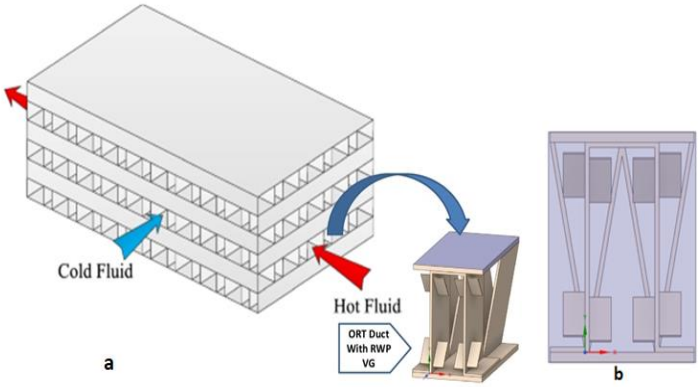

Fig. 1. (a) OSF rectangular-triangular fin(ORT) with RWP VG (b) Front view ORT fin with RWP

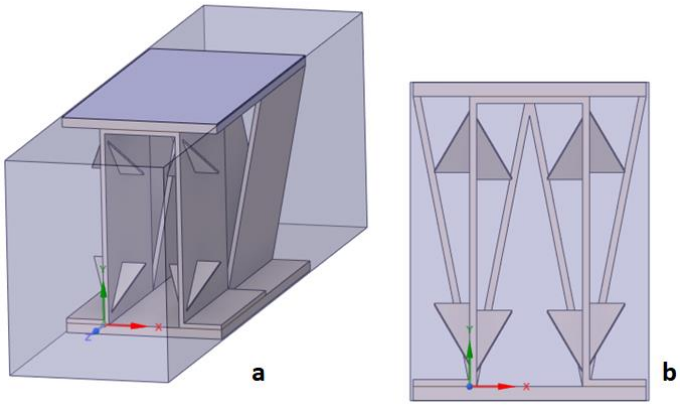

Fig. 2. (a) OSF rectangular-triangular fin(ORT) with DWP VG (b) Front view ORT fin with DWP

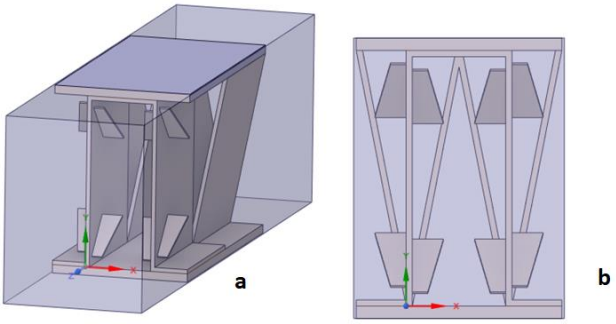

Fig. 3. (a)OSF rectangular-triangular fin(ORT) with TWP VG (b) Front view ORT fin with TWP

Table 1
The detailed description for ORT fin geometry [1]

Fin shape	Fin height, *h* (mm)	Fin space, *s* (mm)	Fin thickness, *t* (mm)	Interrupted length, *l* (mm)	Hydraulic diameter *D* (mm)
proposed Case by Brockmeier *et al.,* [1] (ORT)	10.25	4	0.25	8	3.557

3. Mathematical and Numerical Analysis

3.1 Assumptions

The proposed model solution is simplified on the following presumptions:

i) Three-dimensional model
ii) The air is the working fluid.
iii) A constant properties fluid.
iv) Steady-state flow.
v) The flow is incompressible.
vi) Neglected gravity effect.
vii) Non-slip flow is assumed.
viii) The airflow is laminar, and a laminar model was used.
ix) Neglecting the dissipation of heat is assumed.
x) The wall thickness is neglected

3.2 Governing Equations

By resolving the average differential equation of the momentum equation and continuity equation, the laminar incompressible stable equations may be used to describe the fluid motion in the plate-fin heat exchanger for the laminar state:

3.2.1 Continuity equation

The mass conservation is mathematically represented by the continuity equation. Its form is [14]:

$$\frac{\partial U}{\partial x}+\frac{\partial V}{\partial y}+\frac{\partial W}{\partial z}=0 \tag{1}$$

$$\frac{\partial u}{\partial x}+\frac{\partial v}{\partial y}+\frac{\partial w}{\partial z}=0 \tag{2}$$

3.2.2 Momentum equations (NSEs)

Equations of momentum are a group of equations that are derived from Newton's second law of momentum to conserve the fluid momentum in the three directions of fluid motion; x, y and z [15]. These equations are known as Navier-Stokes equations (NSE), named after Navier and Stokes [16]:

Momentum equation in x-direction:

$$\rho\left(u\frac{\partial u}{\partial x}+v\frac{\partial u}{\partial y}+w\frac{\partial u}{\partial z}\right)=-\frac{\partial p}{\partial x}+\left(\frac{\partial^2 u}{\partial x^2}\right)+\left(\frac{\partial^2 u}{\partial y^2}\right)+\left(\frac{\partial^2 u}{\partial z^2}\right) \quad (3)$$

Momentum equation in y-direction:

$$\rho\left(u\frac{\partial v}{\partial x}+v\frac{\partial v}{\partial y}+w\frac{\partial v}{\partial z}\right)=-\frac{\partial p}{\partial x}+\left(\frac{\partial^2 v}{\partial x^2}\right)+\left(\frac{\partial^2 v}{\partial y^2}\right)+\left(\frac{\partial^2 v}{\partial z^2}\right) \quad (4)$$

Momentum equation in z-direction:

$$\rho\left(u\frac{\partial w}{\partial x}+v\frac{\partial w}{\partial y}+w\frac{\partial w}{\partial z}\right)=-\frac{\partial p}{\partial x}+\left(\frac{\partial^2 w}{\partial x^2}\right)+\left(\frac{\partial^2 w}{\partial y^2}\right)+\left(\frac{\partial^2 w}{\partial z^2}\right) \quad (5)$$

3.2.3. Energy equation

$$u\frac{\partial T}{\partial x}+v\frac{\partial T}{\partial y}+w\frac{\partial T}{\partial z}=\frac{k}{\rho C_p}\left[\frac{\partial^2 T}{\partial x^2}+\frac{\partial^2 T}{\partial y^2}+\frac{\partial^2 T}{\partial z^2}\right] \quad (6)$$

3.3 Boundary Conditions

The inlet velocity for air (cold fluid) was uniform with a temperature of 300k and an outlet pressure equal to zero. Furthermore, the upper and lower plates of the plate-fin heat exchanger were kept at a constant heat flux of (q=3000W/m^2). To facilitate simulation, periodic boundary conditions were adopted for the left and right sides of the computational domain. Finally, the velocity at the walls is assumed to be zero (no slip).

3.4 Hydrodynamic Parameters

The required outcomes have been found by using the "Area Weighted Averaged", "wall flux", and "interfaces" in a sequence for calculating Nu, Q, h, Δp.

For pressure drop, since the outlet is set to pressure zero, the pressure drop is equal to the pressure at the inlet.

Pin - Pout = ΔP

While "volume weighted Averaged", "mass", and "fluid" are used in a sequence to calculate the mean velocity (u) and density ($\boldsymbol{\rho av}$).

The Reynolds number, which is commonly used to explain flow phenomena, is determined by four variables: the flow diameter, as well as the fluid's viscosity, density, and average liner velocity. Eq. (7) defines the Reynolds number [17]:

$$\text{Re} = \rho\, U_{in} D_h/\mu \quad (7)$$

Where $\mathbf{D_h}$ is the hydraulic diameter which is One of the important parameters characterizing the flow in ducts or tubes is the hydraulic diameter. This is used with fluid properties and REs number to calculate inlet velocity

$$D_h = \frac{4A_c}{P_{er}} = \frac{4A_cL}{A} \quad (8)$$

where L is the total length of the plate-fin channel, A is the total heat-transfer area, and Ac is the free flow area in the cross-section.

The Nusselt number: The Nu-number on the heated tube is defined as [18]:

$$\text{Nu}=\frac{1}{A_{(x,z)}} \int_0^l \int_0^w Nu\, dzdx \quad (9)$$

$$Nu = \frac{h\, D_h}{k} \quad (10)$$

Where (h): is the actual average gas-side heat-transfer coefficient

Friction coefficient: The definition of the friction coefficient in terms of shear stress at the channel surface is as:

$$\mathrm{C_f} = \tau_\mathrm{w} /\frac{1}{2}\rho \mathrm{U}^2 \quad (11)$$

Where τ_w the wall is shear stress and defined as:

$$\tau_\mathrm{w} = \mu\sqrt{(\frac{\partial \mathrm{u}}{\partial \mathrm{y}})^2 + (\frac{\partial \mathrm{w}}{\partial \mathrm{y}})^2} \quad (12)$$

Additionally, the friction factor (Fanning fraction factor) is provided by

$$\mathrm{c_f} = \frac{\mathrm{f}}{4} \quad (13)$$

Colburn (j) factor: a dimensionless term, is a function of the Pr-number and the Re-number. It is crucial for figuring out the fluid's heat-transfer coefficient. The source of the J-factor is:

$$\mathrm{j} = \mathbf{St}\, \mathrm{Pr}^{2/3} = \frac{\mathrm{h}}{\rho \mathrm{u} \mathrm{C_p}}\, \mathrm{Pr}^{2/3} \quad (14)$$

Additionally, this component aids in the different correlations that researchers have built to assess the fluid flow parameters, where (St) is the Stanton number**.**

Performance evaluation criterion (PEC) : In order to compare the performance of the PFHE the PEC is studied as a measure of the amount of the heat-transfer enhancement against the pressure drop [19]. The PEC factor is a the larger the better parameter.

$$\mathrm{PEC} = \frac{\mathrm{Nu}/\mathrm{Nu_o}}{\left(\mathrm{f}/\mathrm{f_o}\right)^{1/3}} \quad (15)$$

where $\mathrm{Nu_o}$ and $\mathrm{f_o}$ are the average Nu-number and friction factor for the plane duct.

3.5 Grid Independency

To select the optimal grid and obtain a better solution, a grid independence study is prepared. The investigation of grid independence is taken into account in the current results of seven different values. Table 2 provides a summary of the specified grid for all shapes. At Re = 600, the f-factor is calculated for each arrangement. It is discovered that the value of the f-factor has barely changed. The grid resolution investigation reveals that ORT fin with RWP, with DWP, and with TWP become independent of the grid at cells1 86213, 151214, and 182214 cells respectively.

Table 2
Different studied cases and them different grids with their f-factor results.

No.	Case	No. of grid elements	f	$f_{deviation}$
1	ORT with RWP of (en=0.5mm, h=1.25mm and β=45°)	65012	0.118822731	0.016661257
		82986	0.116842995	0.104373523
		113658	0.10464768	0.020730894
		186213	0.10247824	0.0009523
		292682	0.10238065	0.002371347
		622526	0.10213787	0.00113337
		1211330	0.10202211	
2	ORT with DWP of (en=0.5mm, h=1.25mm and β=45°)	61010	0.122822732	0.105678613
		72986	0.109842996	0.019985944
		111657	0.10764768	0.020153151
		182214	0.10547824	0.000925215
		281681	0.10538065	0.002303839
		682526	0.10513787	0.00110103
		9201330	0.10502211	
3	ORT with TWP of (en=0.5mm, h=1.25mm and β=45°)	65012	0.118822731	0.016661257
		82986	0.116842995	0.104373523
		113658	0.10464768	0.020730894
		186213	0.10247824	0.0009523
		292682	0.10238065	0.002371347
		622526	0.10213787	0.00113337
		1211330	0.10202211	

3.6 Solving by FLUENT

The commercial (CFD) code can be used to solve the numerical method of the discredited governing equations. ANSYS Fluent 2021 R1 is the program uses to calculate the current numerical investigation. Fluent is frequently used in this field and it is regarded as some of the best code currently in use [20]. The governing equations are approximated using a laminar model and finite volume discretization. The numerical computation employs a pressure-based solver with double precision. On the PFHE surface, a non-slip boundary condition is used. For pressure velocity coupling, the SIMPLE method is employed. The discretization of all terms was done using a second-order upwind approach.

3.7 Validations

Through this work the J-factor values for the OSF fin in the PFHE are established numerically, for the experimental works of Yang *et al*., [21] . The validations including the J-factor are displayed in Figure 4. The average deviation for the J-factor between the experimental works of Yang *et al*., [21] and the numerical work is 3% which shows a good agreement.

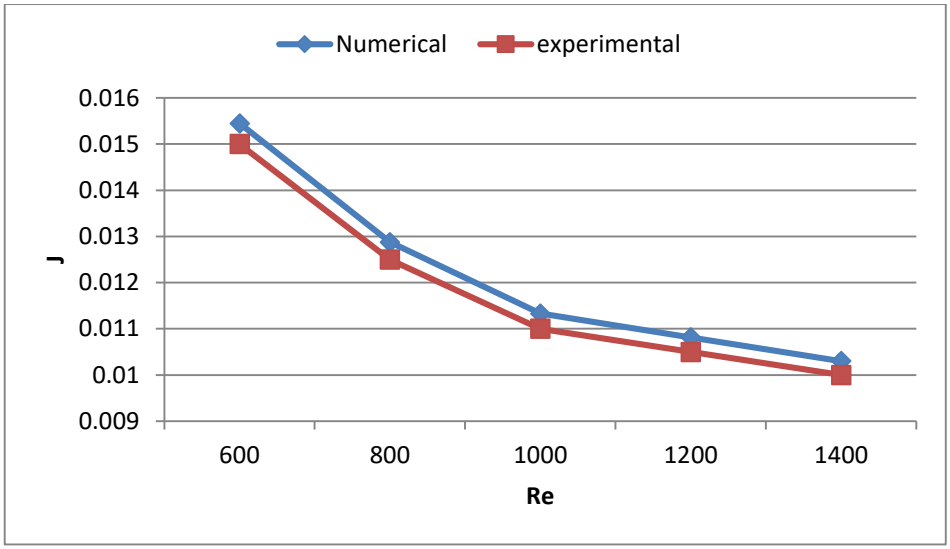

Fig. 4. Comparison of the numerical values and the experimental data of J-factor(J) air tests for Yang *et al*., [21]

4. Results and Discussion

The numerical results in this section have been addressed to verify the strengthening of forced convection in a PFHE with different fin configurations and with aid of a vortex generator. The studied cases for PFHE of the ORT fin with different vortex generator are discussed.

4.1 Performance Analysis of PFHE with Aid of the RWP Longitudinal Vortex Generator
4.1.1 Effect of varying entrance length on the LVG
4.1.1.1 Nusselt number

Figure 5 displays The effect of varying the entrance length on the LVG on the average Nusselt number variation for laminar RE number Re = 600 and the optimum angle of attack and height (β=45° and h=1.25mm)

The calculations are achieved at three different locations of the RWP LVG. From the inlet, the distance of the leading edge of the LVG is varied, i.e., L = 0.25, 0.5, 3 and 5mm. As the RWP is moved towards the inlet of the fin, the influence range of the LV gets larger in the streamwise direction, so the Nusselt number and the coefficient of heat-transfer reach their optimum values for the entrance length L = 0.5mm. Figure 5 shows the average value of Nu-number of RWP LVG at L = 0.5mm is 14.85% higher than the ORT fin without using the VG, for laminar RE number Re = 600 and the optimum angle of attack and height (β=45° and h=1.25mm).

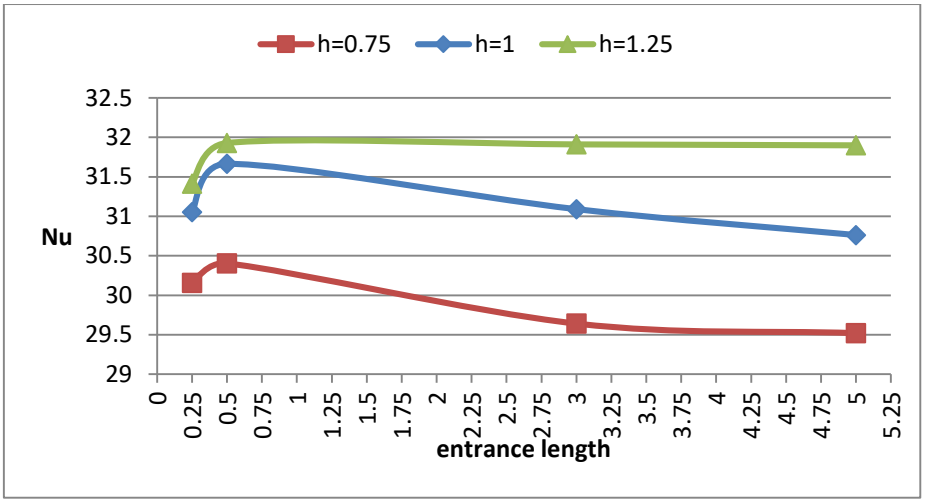

Fig. 5. Effect of entrance length and VG height on Nusselt number at β= 45° and Re = 600

4.1.1.2 Pressure Loss

The heat-transfer enhancement is combined with an enlarged pressure loss, this can be attributed to the fact that the flow is obstructed by the WPVG thus the pressure loss increases. But in many applications, the heat-transfer augmentation is more significant even at the additional pumping cost [13].

The influence of varying the entrance length on the LVG on the average Pressure Loss variation for laminar RE number Re = 600 and the optimum angle of attack and height (β=45° and h=1.25mm) is illustrated in Figure 6.

The calculations are carried out at three different locations of the RWP LVG, i.e. L = 0.25, 0.5, 3 and 5mm. As the RWP LVG is moved downstream of the fin, the influence Pressure Loss ranges get larger slightly, so the Pressure drop reaches its optimum values for the entrance length L = 0.5mm. Figure 6 shows the value of pressure drop of RWLVG at l = 0.5mm is 48.95% higher than the ORT fin without using the VG for laminar RE number Re = 600 and angle of attack and height (β=45° and h=1.25mm)

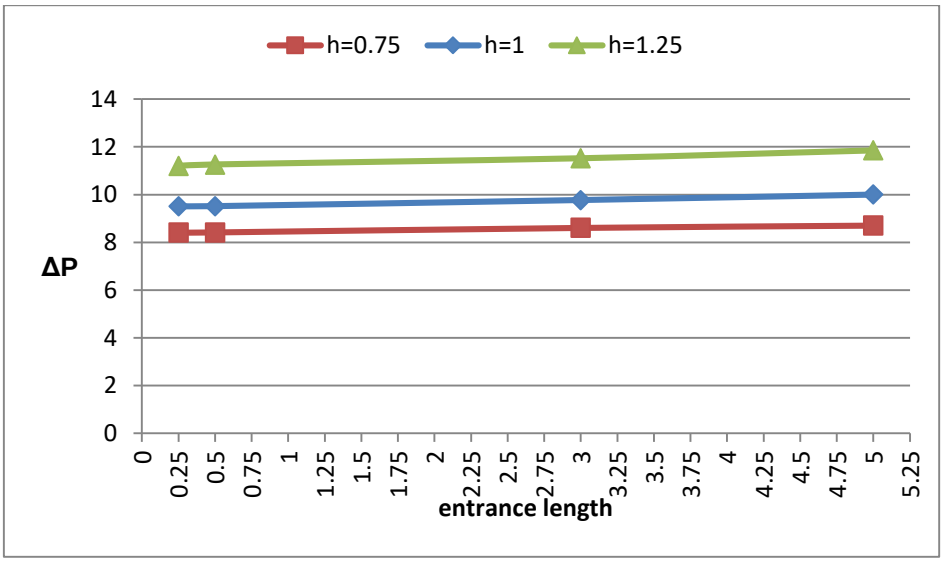

Fig. 6. Effect of entrance length and VG height on pressure drop at β= 45° and Re = 600

4.1.2 Effect of varying the Reynold number on the LVG

4.1.2.1 Nusselt number

The effect of varying the Re-number of the LVG on the average Nu-number variation for the optimum angle of attack, height and entrance length (β=45°, h=1.25mm, L=0.5mm) is shown in Figure 7.

The computations were performed at a laminar Reynolds Re = 600, 800, 1000,1200 and 1400, which shows that the percentage of heat-transfer enhancement increases as the REs increase, since at a higher Re-number the mass flow rate is greater, then more heat removal takes place. Also at a higher RE the thermal boundary layer thickness decreases and the degree of fluid mixing increases. So, the heat-transfer increases with the increase in the Re [8]. The results show that the Nu-number reaches its optimum enhancement values for the Re-number Re = 1400 by 22.23% of RWP LVG higher than the ORT fin without using the VG.

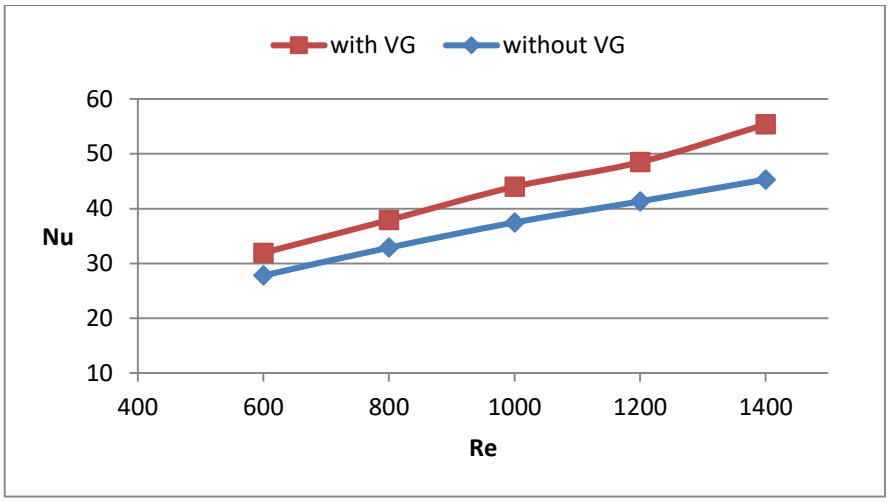

Fig. 7. Effect of Reynold number with the LVG of (β=45°, h=1.25mm, en=0.5mm) on the Nusselt number

4.1.2.2 Pressure loss

Increasing the Re-number increases the inertia forces, thus the pressure drop is increased by increasing the Re number. Figure 8 demonstrated The effect of varying the RE number of the LVG on the average Pressure Loss variation for the optimum angle of attack, height and the entrance length (β=45°, h=1.25mm, L=0.5mm).

The computations were performed at a laminar Reynolds Re = 600, 800, 1000,1200 and 1400, which displays that the percentage of Pressure Loss increases as the REs increase which was agreed with previous studies [2, 7]. The results show that Pressure Loss reaches its peak values for the Re-number = 1400 by 44.69 % of RWP LVG higher than the ORT fin without using the VG.

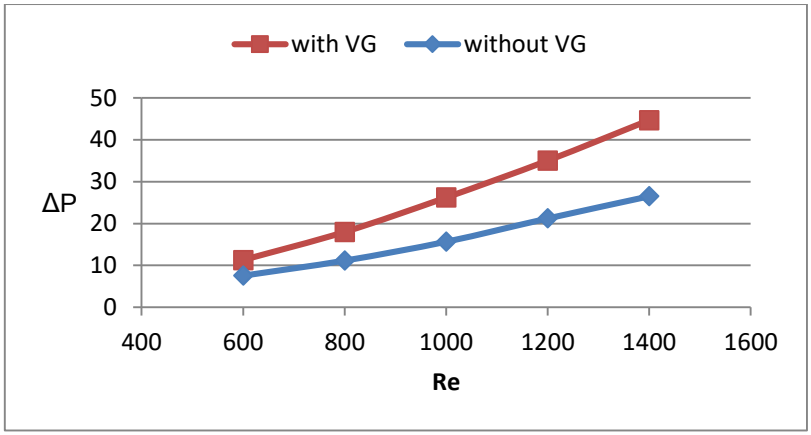

Fig. 8. Effect of Reynolds number with the LVG of (β=45°, h=1.25mm, L=0.5mm) on the pressure drop

4.2 Performance Analysis of PFHE with Aid of the Various Types of Vortex Generator

In addition to the RWP VG, two more types of VG where examined in there thermo-hydraulic features which are the delta winglet pair (DWP) and trapezoidal winglet pair (TWP)

4.2.1 Nusselt number

The effect of varying the RE number of the various types LVG on the average Nusselt number variation for the optimum angle of attack, height and the entrance length (β=45°, h=1.25mm, L=0.5mm) is showed in Figure 9 The results show that ORT with RWP have the highest value of Nusselt number thus the heat-transfer enhancement. While the TWP and the DWP come in the 2nd and 3rd place, respectively.

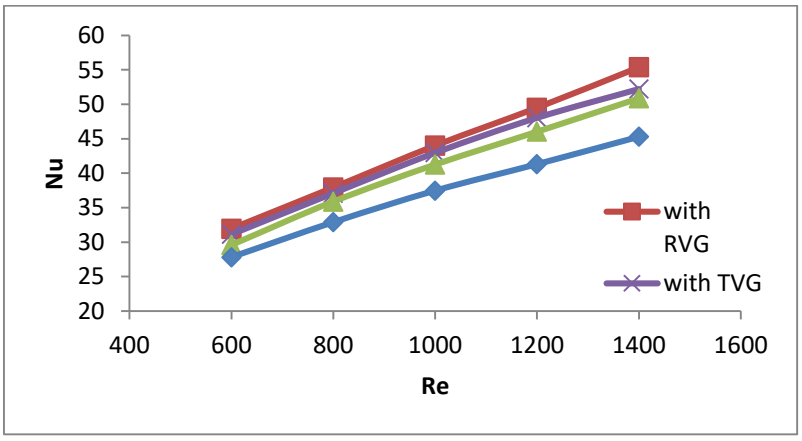

Fig. 9. Effect of Reynold number with various types of vortex generator of (β=45°, h=1.25mm, L=0.5mm) on the Nusselt number

4.2.2 Pressure loss

The creation of vortexes causes the flow to diverge from its main path, which is the main contributor to the increased pressure loss by using vortex generator. In fact, the greater is the effect of the VG on the heat transfer, the greater is the pressure loss [22]. Figure 10 demonstrated the effect of varying the RE number of the various types LVG on the average Pressure Loss variation for the optimum angle of attack, height and the entrance length (β=45°, h=1.25mm, L=0.5mm). the figure

displays that the DWP have the least pressure drop as compared with the other VGs. The pressure drop increases with increase of REs number, and the difference between the three types also growths.

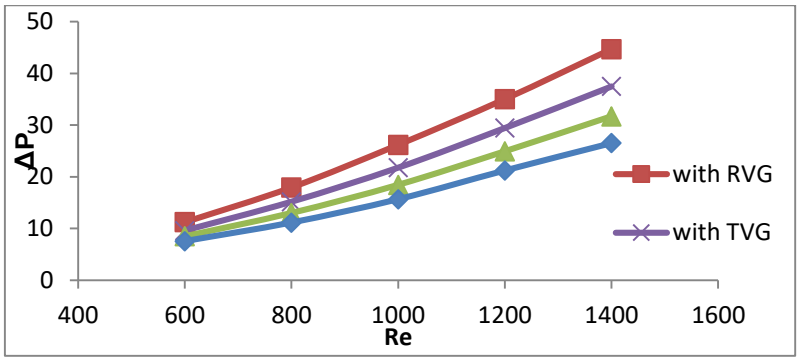

Fig. 10. Effect of Reynold number with various types of vortex generator of (β=45o, h=1.25mm, L=0.5mm) on the Pressure drop

4.3 Performance Evaluation Criterion (PEC)

The use of VG improves the heat-transfer, and also increases the pressure loss. In order to compare of the PFHE performance, a performance evaluation criterion (PEC) is considered as a measure of the amount of the heat-transfer augmentation against the pressure loss [23]. Table 3 explains in detail the PEC values for various LVG of (β=45°, h=1.25mm, L=0.5mm) as compared with the ORT fin without VG as the reference surface. A greater PEC values means the system is more economical. The table shows that the rectangular vortex generator (RWP) with a higher PEC values has the best performance and is the most efficient vortex generator. It is found that, however the heat-transfer enhancement in channels with TWP is more than channels with DWP, the PEC of the channels with DWP is better than channels with TWP. It is observed that the value of the PEC increases with the increase in the REs number

Table 3
PEC values for different VG at a different values of Reynolds number.

Re	PEC		
	RWP	DWP	TWP
600	1.051	1.0501914	0.9882446
800	1.033225	1.0326869	0.9998653
1000	1.046216	1.0444706	0.9946914
1200	1.052174	1.048322	1.0063242
1400	1.125463	1.0882313	1.0700337

4.4 Thermal Characteristic

4.4.1 Thermal characteristic of PFHE with aid of the longitudinal vortex generator

This section deals with the temperature variation along the domain of ORT fin in a PFHE with aid of the LVG of (β=45°, h=1.25mm, L=0.5mm and Re=600), a temperature contour has been captured as shown in Figure 11 And Figure 12, for the ORT fin without and with RWP VG, respectively. The frame b, c and d illustrate the section of the domain at L=4mm, L=8mm and L=12mm, respectively. where the outlet temperature of the domain increases concerning the flowing downstream. As shown in temperature distribution figures, there is a reduction in the internal cold area in the fluid

domain as a result of using the modified ORT fin configuration on which the vortex generators are mounted, as represented by the dark blue fluid colour entering the domain. As it's shown in the figures below, the blue area reduced as well as the heat-transfer enhanced between the fins and the flowing fluid. The longitudinal vortices facilitate the exchange of fluid near the walls with the fluid in the core and hence the boundary layer is disturbed. It causes an increase in temperature gradient at the surface which leads to the augmentation in heat-transfer.

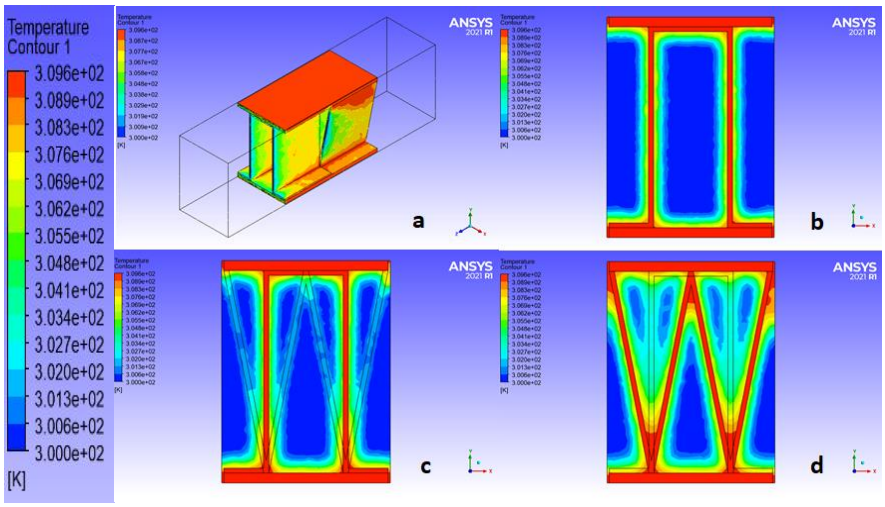

Fig. 11. Temperature distribution for ORT fin for Re=600. (a) fluid domain in contact with the fin (b) section of the domain at l=4mm (c) section of the domain at l=8mm (d) section of the domain at l=12mm [1]

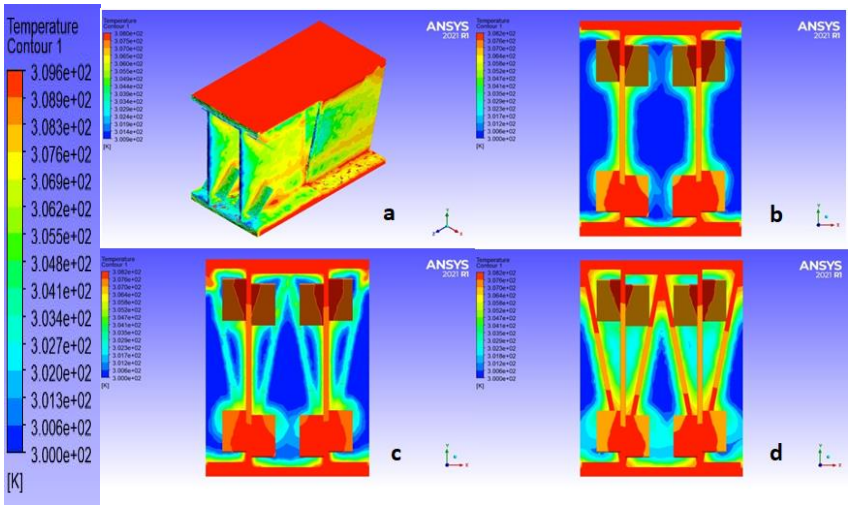

Fig. 12. Temperature distribution for ORT fin with aid of the LVG of (β=45°, h=1.25mm, L=0.5mm) for Re=600. (a) fluid domain in contact with the fin (b) section of the domain at L=4mm (c) section of the domain at L=8mm (d) section of the domain at L=12mm

4.4.2 Stream Line

Figure 13 presents the streamline for the case of ORT fin geometry and the ORT with aid of the LVG of (β=45°, h=1.25mm and L=0.5mm) of the PFHE, for air flowing with Re = 600, while the Figure 14 of the frames a, b, c, d, e and f, illustrate the streamline for a different section of the domain at L=0mm, L=2mm, L=3mm, L=4mm, L=8mm, and L=12mm, respectively.

As it's displayed from the figures the area near the triangle corners is poorer from the heat-transfer point, which is realized from the red colour of the contour, and by using the pair of the VG and each part of the pair closer and at the same line of these corners the longitudinal vortices increases the heat enhancement in these parts since swirling motions generated by flow separation behind edges of winglet VG are the main reason of the heat-transfer coefficient enhancement. Also, the boundary layer gets disturbed and fluid mixes from the core cold region to the hot region near the walls by using the LVG leading to the enhancement of heat-transfer.

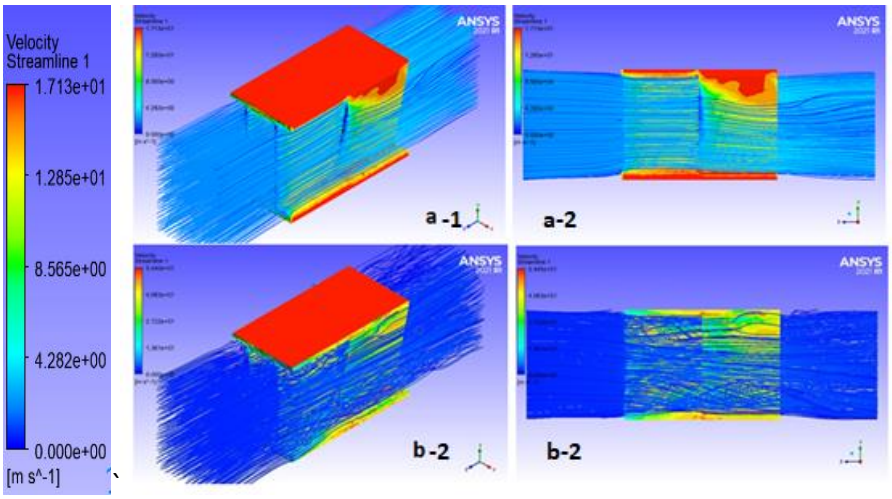

Fig. 13. Stream lines for ORT fin.(a) without LVG (b) with aid of the LVG

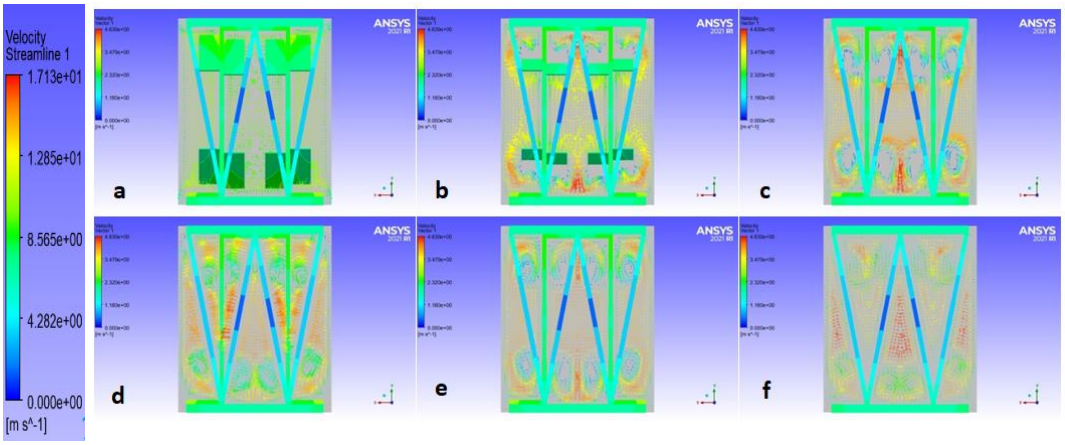

Fig. 14. Stream lines for ORT fin. (a) L=0mm (b) L=2mm (c) L=3mm (d) L=4mm (e) L=8mm (f) L=12mm

5. Conclusions and Future Work

In this paper, a numerical thermo-dynamic fluid model is established which can predict the flow and heat transfer characteristics at laminar Re-number, furthermore has dealt with heat transfer enhancement in PFHE of the novel combination (ORT) fins with RWP type longitudinal VG. The computational study has been done to determine the flow and heat transfer characteristics for different height and leading edges of RWP. Finally, a two more LVG are tested with the optimum conditions of the RWP, which they are a (DWP) and (TWP). A good agreement was accomplished between the experimental data of Yang *et al*., [21] and numerical predictions for the j-factor.

The major conclusions are summarized as follows:

1- Compared with the base case configuration, the Common flow up (CFU) vortex generator configuration with RWP LVG at attack angle, height and entrance length (β=45°, h=1.25mm, L=0.5mm) gives a maximum heat transfer rate.
2- The convective heat transfer was improved by the longitudinal vortices, not only in the region near LVGs but also in the large region downstream. So by decreasing the entrance length of the LVG to its optimal value (L=0.5mm) it can enhance the global heat-transfer of the PFHE.
3- The pressure drop in the PFHE flow with ORT fin configuration when the RWP is mounted on the rectangular surface of the fin side, increases slightly by increasing the entrance length.
4- At higher Re-number, the mass flow rate increases hence higher heat removal takes place. So, the heat-transfer increases with the rise in the Re-number. The results show that Nu-number reaches its optimum enhancement values for the Re-number Re = 1400 by 22.23% of RWP higher than the ORT fin without using the vortex generator.
5- Although the heat transfer rate is enhanced because of the RWP leading to a more compact in heat exchanger, there is an associated increase in the pumping power. It can be seen that about 14.85-22.23% enhancement of heat-transfer can be achieved at the income of a moderate pressure drop by 48.94-68.46%.
6- Increasing the height of the VGs increases its effect on improving the heat-transfer for all angles of attack and entrance lengths
7- With an increase in the attack angle, height and Re-number the percentage of heat transfer enhancement concerning the base case configuration increases for all common flow up (CFU) configurations.
8- As compared with the DWP and TWP, The RWP vortex generator have a highest Nussult number and PEC values thus the best performance and the most efficient vortex generator.
9- The shape of primary vortices caused by the RWP are maintained over a long distance in downstream, but the strength of the primary vortices decreases as the vortices develop in downstream region of the PFHE.

A recommendations for future work could be to investigate the thermal and hydro-dynamic fields of the fourth proposed case by Brockmeier *et al.,* [1] which was the PFHE with offset triangular fin (OT), by mounting the same vortex generator presented in this paper on the fin surface.

References

[1] Brockmeier, U., T. H. Guentermann, and M. Fiebig. "Performance evaluation of a vortex generator heat transfer surface and comparison with different high performance surfaces." *International journal of heat and mass transfer* 36, no. 10 (1993): 2575-2587. https://doi.org/10.1016/S0017-9310(05)80195-4
[2] Abed, Ammar A., and Wissam H. Khalil. "A Numerical Study of the Heat Transfer and Fluid Flow in Different Shapes of Microchannels." *Al-Nahrain Journal for Engineering Sciences* 19, no. 1 (2016): 66-75.
[3] Gupta, M., K. S. Kasana, and R. Vasudevan. "A numerical study of the effect on flow structure and heat transfer of a rectangular winglet pair in a plate fin heat exchanger." *Proceedings of the Institution of Mechanical Engineers, Part C: Journal of Mechanical Engineering Science* 223, no. 9 (2009): 2109-2115. https://doi.org/10.1243/09544062JMES1405
[4] Ganesh, N., Hema Kumar Theertham, and Sundararaj Senthilkumar. *Heat Transfer Augmentation of Compact Plate Fin Heat Exchanger Using Modified Fin Surfaces*. No. 2018-28-0012. SAE Technical Paper, 2018. https://doi.org/10.4271/2018-28-0012
[5] Ebrahimi, Amin, and Saeid Kheradmand. "Numerical simulation of performance augmentation in a plate fin heat exchanger using winglet type vortex generators." *International Journal of Mechanical Engineering and Mechatronics* 1, no. 2 (2012): 109-121. https://doi.org/10.11159/ijmem.2012.014

[6] Gupta, Munish, K. S. Kasana, and R. Vasudevan. "Heat transfer augmentation in a plate-fin heat exchanger using a rectangular winglet." *Heat Transfer—Asian Research* 39, no. 8 (2010): 590-610. https://doi.org/10.1002/htj.20318
[7] Khoshvaght-Aliabadi, Morteza. "Thermal performance of plate-fin heat exchanger using passive techniques: vortex-generator and nanofluid." *Heat and Mass Transfer* 52, no. 4 (2016): 819-828. https://doi.org/10.1007/s00231-015-1603-6
[8] Vasudevan, R., V. Eswaran, and G. Biswas. "Winglet-type vortex generators for plate-fin heat exchangers using triangular fins." *Numerical Heat Transfer: Part A: Applications* 38, no. 5 (2000): 533-555. https://doi.org/10.1080/104077800750020423
[9] Sachdeva, Gulshan, K. S. Kasana, and R. Vasudevan. "Heat transfer enhancement by using a rectangular wing vortex generator on the triangular shaped fins of a plate-fin heat exchanger." *Heat Transfer—Asian Research: Co-sponsored by the Society of Chemical Engineers of Japan and the Heat Transfer Division of ASME* 39, no. 3 (2010): 151-165. https://doi.org/10.1002/htj.20285
[10] Sachdeva, Gulshan, R. Vasudevan, and K. S. Kasana. "Computation of heat transfer enhancement in a plate-fin heat exchanger with triangular inserts and delta wing vortex generator." *International journal for numerical methods in fluids* 63, no. 9 (2010): 1031-1047. https://doi.org/10.1002/fld.2113
[11] Gupta, M., and K. S. Kasana. "Numerical study of heat transfer enhancement and fluid flow with inline common-flow-down vortex generators in a plate-fin heat exchanger." *Heat Transfer—Asian Research* 41, no. 3 (2012): 272-288. https://doi.org/10.1002/htj.20414
[12] Khalaf, Abbas Fadhil, Farhan Lafta Rashid, Ali Basem, and Mohammed H. Abbas. "Mathematical Modelling of Engineering Problems." *Journal homepage: http://iieta. org/journals/mmep* 9, no. 6 (2022): 1639-1647. https://doi.org/10.18280/mmep.090532
[13] Samadifar, Mohammad, and Davood Toghraie. "Numerical simulation of heat transfer enhancement in a plate-fin heat exchanger using a new type of vortex generators." *Applied Thermal Engineering* 133 (2018): 671-681. https://doi.org/10.1016/j.applthermaleng.2018.01.062
[14]] H. Mahdi. Numerical and Experimental study of Enhancement of heat transfer in Roughened Ribbed Duct. PHD thesis, Department of technical Eduction, University of technology, Iraq, 2004.
[15] Versteeg, H. K., and W. Malalasekera. "An introduction to Computational Fluid Dynamics Prentice Hall." (1995).
[16] Saysroy, A., and S. Eiamsa-Ard. "Enhancing convective heat transfer in laminar and turbulent flow regions using multi-channel twisted tape inserts." *International Journal of Thermal Sciences* 121 (2017): 55-74. https://doi.org/10.1016/j.ijthermalsci.2017.07.002
[17] Nabil, Rand, and Ali Sabri. "A review on the modification of circular fin and tube heat exchangers through new innovative fin shapes." *International Journal of Advanced Technology and Engineering Exploration* 9, no. 93 (2022): 1222. https://doi.org/10.19101/IJATEE.2021.875888
[18] Abbas, Noor Y., Ahmed W. Mustafa, and Mohammed Kheir Aldeen Abbas Askera. "Constructal Design of Heat Exchangers: A Review." *International Journal of Advances in Engineering and Management* 3: 27-40.
[19] Abbas, Ali Sabri, and Ayad Ali Mohammed. "Enhancement Of Plate-Fin Heat Exchanger Performance with Aid of Various Types of Fin Configurations: A Review." *Journal of Advanced Research in Fluid Mechanics and Thermal Sciences* 99, no. 2 (2022): 48-66. https://doi.org/10.37934/arfmts.99.2.4866
[20] Fluent Corp., Fluent 2021 R1 User Guide Manual, Fluent Press, New Hampshire, 2021.
[21] Yang, Huizhu, Jian Wen, Simin Wang, and Yanzhong Li. "Effect of fin types and Prandtl number on performance of plate-fin heat exchanger: Experimental and numerical assessment." *Applied Thermal Engineering* 144 (2018): 726-735. https://doi.org/10.1016/j.applthermaleng.2018.08.063.
[22] Niknahad, Ali. "Numerical study and comparison of turbulent parameters of simple, triangular, and circular vortex generators equipped airfoil model." *Journal of Advanced Research in Numerical Heat Transfer* 8, no. 1 (2022): 1-18.
[23] Shlash, Bassam Amer Abdulameer, and Ibrahim Koç. "Turbulent fluid flow and heat transfer enhancement using novel Vortex Generator." *Journal of Advanced Research in Fluid Mechanics and Thermal Sciences* 96, no. 1 (2022): 36-52. https://doi.org/10.37934/arfmts.96.1.3652.